Journal of Power Sources 185 (2008) 1348–1353

Contents lists available at ScienceDirect

Journal of Power Sources

journal homepage: www.elsevier.com/locate/jpowsour

# Semiempirical model based on thermodynamic principles for determining 6 kW proton exchange membrane electrolyzer stack characteristics

N.V. Dale[a,*], M.D. Mann[a], H. Salehfar[b]

[a] Chemical Engineering Department, University of North Dakota, Grand Forks, ND 58202, USA
[b] Electrical Engineering Department, University of North Dakota, Grand Forks, ND 58202, USA

ARTICLE INFO

*Article history:*
Received 25 June 2008
Received in revised form 1 August 2008
Accepted 20 August 2008
Available online 28 August 2008

*Keywords:*
PEM electrolysis
Reversible potential
Exchange current density
Membrane conductivity

ABSTRACT

The performance of a 6 kW proton exchange membrane (PEM) electrolyzer was modeled using a semiempirical equation. Total cell voltage was represented as a sum of the Nernst voltage, activation overpotential and ohmic overpotential. A temperature and pressure dependent Nernst potential, derived from thermodynamic principles, was used to model the 20 cell PEM electrolyzer stack. The importance of including the temperature dependence of various model components is clearly demonstrated. The reversible potential without the pressure effect decreases with increasing temperature in a linear fashion. The exchange current densities at both the electrodes and the membrane conductivity were the coefficients of the semiempirical equation. An experimental system designed around a 6 kW PEM electrolyzer was used to obtain the current–voltage characteristics at different stack temperatures. A nonlinear curve fitting method was employed to determine the equation coefficients from the experimental current–voltage characteristics. The modeling results showed an increase in the anode and cathode exchange current densities with increasing electrolyzer stack temperature. The membrane conductivity was also increased with increasing temperature and was modeled as a function of temperature. The electrolyzer energy efficiencies at different temperatures were evaluated using temperature dependent higher heating value voltages instead of a fixed value of 1.48 V.



## 1. Introduction

The problems associated with fossil fuels including the world's growing dependency on it have necessitated the search for an alternative. Hydrogen is an attractive alternative and is seen by many as an excellent energy carrier for the future. Hydrogen's high specific enthalpy of combustion makes it a potential candidate for transportation. Hydrogen can typically be generated either from fossil fuels or from water by utilizing electrical energy. Though hydrogen is a clean fuel, significant emissions are generated when hydrogen is produced from fossil fuels, its most common form of production. Hydrogen generation through water electrolysis from renewable energy is more environmentally friendly, but it is not yet a cost competitive method compared to other technologies. NREL's milestone report suggests that 80% of the total selling price of hydrogen from large scale electrolyzes is comprised of electricity cost [1]. Therefore, improvement in the electrical energy efficiency of the electrolyzers is of prime importance. For hydrogen production, the electrical energy efficiency of electrolyzers is more important than the heat energy efficiency [2]. The electrical energy efficiency can be improved by reducing the reversible voltage, activation losses and ohmic losses.

Among the available technologies for water electrolysis, proton exchange membrane (PEM) electrolysis has advantages of high electrolyzing efficiency at higher current densities and hydrogen purity [3]. The cell voltage of a PEM electrolyzer can be described as the sum of Nernst voltage, anode and cathode overpotentials and the overpotential due to the membrane resistance. The Nernst overpotential is dependent on the change in Gibbs' free energy during the reaction, the pressure, and concentrations of the reactants and products. Gibbs' free energy changes with the temperature, however, many investigators assume a constant reversible potential ($E^0_{rev}$) value of 1.23 V while modeling the current–voltage characteristic of PEM electrolyzers. In this paper, thermodynamic modeling of the water electrolysis reaction is carried out to establish the dependence of reversible potential on temperature. The Renewable Hydrogen Test Facility at University of North Dakota (UND) has a 6 kW PEM electrolysis system. The

* Corresponding author. Tel.: +1 701 330 2760; fax: +1 701 777 3773.
*E-mail address:* nileshdale@gmail.com (N.V. Dale).

0378-7753/$ – see front matter © 2008 Elsevier B.V. All rights reserved.
doi:10.1016/j.jpowsour.2008.08.054

**Nomenclature**

| | |
|---|---|
| $E$ | cell voltage (V) |
| $F$ | Faraday's constant, 96,485 C |
| $\Delta G$ | change in Gibbs' free energy (J) |
| $G^0_{f,H_2}$ | Gibbs' free energy of formation of hydrogen at 25 °C (J) |
| $G^0_{f,O_2}$ | Gibbs' free energy of formation of oxygen at 25 °C (J) |
| $G^0_{f,H_2O(liq.)}$ | Gibbs' free energy of formation of liquid water at 25 °C (J) |
| $\Delta H$ | change in enthalpy (J) |
| $\Delta H_{t,p}$ | change in enthalpy at $t$ °C and $p$ atm (J) |
| $\Delta H^0_t$ | change in enthalpy at $t$ °C and standard pressure (J) |
| $\Delta H^0_{25}$ | change in enthalpy at 25 °C and standard pressure (J) |
| $j$ | current density (A cm$^{-2}$) |
| $j_{x,o}$ | exchange current density (A cm$^{-2}$) |
| $P_{O_2}$ | partial pressure of oxygen (N m$^{-2}$) |
| $P_{H_2}$ | partial pressure of hydrogen (N m$^{-2}$) |
| $R$ | gas constant (8.314 J mol$^{-1}$ K$^{-1}$) |
| $\Delta S$ | change in entropy (J) |
| $t$ | temperature (°C) |
| $T$ | temperature (K) |
| $V_{HHV,t}$ | higher heating voltage at $t$ °C (V) |
| $V_t$ | enthalpic voltage at $t$ °C (V) |

*Greek letters*

| | |
|---|---|
| $\alpha$ | charge transfer coefficient |
| $\sigma$ | membrane conductivity (S cm$^{-1}$) |
| $\varphi$ | membrane thickness (μm) |

system allows advanced control and monitoring over parameters such as temperature and pressure. This system was used to obtain the *I–V* characteristics at different temperatures.

The temperature dependent value of Nernst potential was evaluated and used to model the experimental *I–V* characteristics of the 6 kW PEM electrolyzer. The anode and cathode overpotentials and ohmic overpotential due to the membrane were modeled using equations reported in the literature [4]. PEM electrolyzer parameters such as membrane thickness, membrane type, conductivity, and exchange current densities are proprietary information and generally are not shared by the manufacturers. Values of these parameters vary from author to author and there is a wide range of values depending on the operating conditions, catalyst loading and the type of electrolyzer stack. These parameters were extracted using a nonlinear curve fitting method and the semiempirical equation, based on temperature dependent Nernst potential, which was developed as part of this work. The temperature dependent Nernst potential will be very useful in predicting a more accurate cell voltage of the PEM electrolyzer. The semiempirical equation can be used in hydrogen system modeling based on renewable energies. The temperature dependent equation for higher heating value voltage will also predict more accurately the energy efficiency of the electrolyzer. This improvement will be realized since the present electrolyzer energy efficiency calculations use a constant higher heating value voltage of 1.48 V.

## 2. Experimental setup

The experimental system at UND is built around Distributed Energy System's (formerly, Proton Energy Systems) 6 kW HOGEN® 40 PEM electrolyzer stack as shown in Fig. 1. The off-the-shelf HOGEN40® stack is rated to produce 1.05 N m$^3$ of dry hydrogen gas at 200 psig (13.8 atm) per hour using de-ionized (DI) water [5]. The PEM stack consists of 20 cells connected in series having an active area of 0.093 ft$^2$ (86.4 cm$^2$) which results in a maximum current density of 1.6 A cm$^{-2}$ at 140 A. The overall system is designed to provide for a precise control of operating temperature, hydrogen system pressure, water resistivity, water flow, stack current, and safety. As shown in Fig. 1, a temperature control unit (chiller) controls the inlet DI water temperature thereby providing control of the operating temperature of electrolyzer. This system is designed to allow higher temperature testing by maintaining the DI water temperature using the chiller and a heater in the oxygen–water phase separator. After achieving the desired resistivity and temperature of DI water, the stack is supplied with power, using two programmable DC power supplies, and DI water is run through the stack. The flow of the DI water to the stack is controlled between 1.5 and 2.5 gal/min. Before entering the stack, DI water goes through a 10 μm filter and sensing stage where its temperature, flow, pressure and resistivity are monitored for a stable and safe operation. Hydrogen gas coming out of the cathode side is separated from liquid water in a high-pressure hydrogen–water separator. A coalescing filter, immediately following the separator, removes most of the remaining liquid water from the hydrogen gas. An automatic drain connected to the coalescing filter collects and recycles the DI water back to the external reservoir with the help of hydrogen system pressure. A two tube desiccant drying system performs the remaining drying process of the hydrogen gas. Dry hydrogen gas then enters the sensing stage equipped with mass flow, temperature, pressure and dew point sensors. A back pressure regulator (BPR) can be adjusted to maintain the hydrogen system pressure. Oxygen from anode side is separated from DI water in the oxygen phase separator where oxygen is then vented out using a check valve and DI water is reused.

Experimental *I–V* characteristics were obtained for different temperatures up to 60 °C by sweeping the input current to the electrolyzer from 1 to 140 A in 1 A steps. The water temperature control unit helps maintain the stack temperature at specified operating temperature throughout the experiment. The system pressure varies with stack input current and was maintained at 145 psi by a back pressure regulator at the stack output.

## 3. Modeling

Using electricity, hydrogen generation is achieved by dissociating water molecules into the diatomic molecules of hydrogen and oxygen. The overall water electrolysis reaction can be represented as

$$H_2O \rightarrow H_2 + \frac{1}{2}O_2 \quad \Delta H^0_{25} = 285.83\,\text{kJ}$$

where $\Delta H^0_{25}$ is the change in enthalpy of the reaction at 25 °C and standard pressure of one atmosphere for liquid water. Electrolysis of 1 mol of water produces 1 mol of hydrogen and a 0.5 mol of oxygen. The bridge between electrical energy and chemical energy needed to carry out the water electrolysis can be represented by Eq. (1)

$$E = -\frac{\Delta G}{nF} \tag{1}$$

where $E$ is the electrolysis cell voltage, $n$ is the number of electrons transferred during the reaction (2 for water electrolysis reaction), $\Delta G$ is the change in Gibbs' free energy of the reaction and $F$ (the Faraday's constant) is 96,485 C.

This fundamental equation gives the electromotive force (emf) or voltage required for water electrolysis assuming no losses or irreversibilities. Thus, the voltage ($E$) needed for water electrolysis

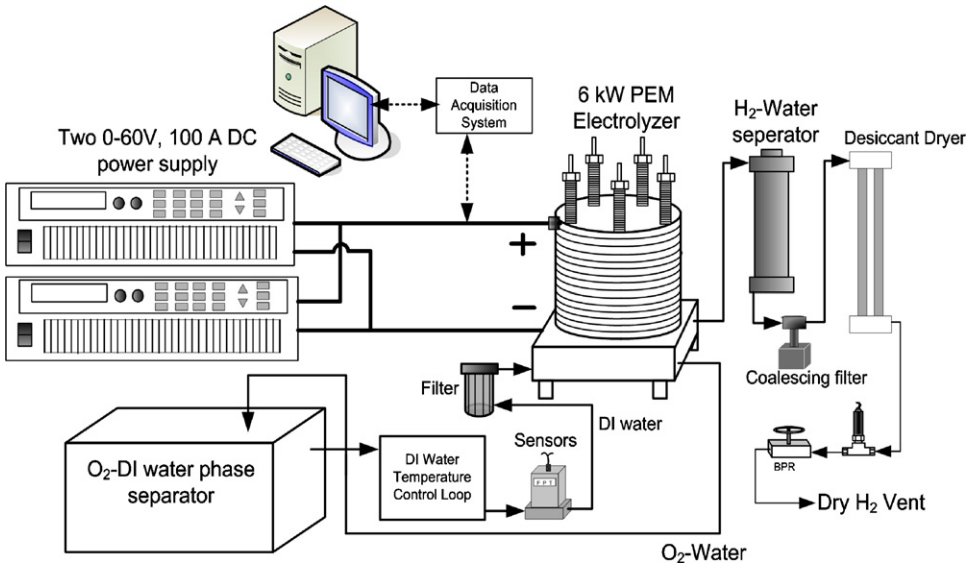


**Fig. 1.** Experimental setup at UND for a 6 kW PEM electrolysis system with temperature control.

is directly proportional to the Gibbs' free energy of the reaction and is represented in Eq. (1). The Gibbs' free energy is in turn dependent on the change in enthalpy ($\Delta H$) of the reaction. Enthalpy is a function of temperature which causes the Gibbs' free energy to vary with temperature, and therefore the potential ($E$) required to carry out the electrolysis reaction is also temperature dependent. While modeling the electrolyzer, dependence of the reversible potential on the temperature is generally ignored. This can result in inaccurate interpretations of the efficiency and electrolyzer cell parameters such as membrane conductivity, anode and cathode exchange densities, and charge transfer coefficients at the electrodes [6]. Many investigators use a value 1.23 V for the reversible potential while modeling an electrolysis cell or stack, which is true only at standard temperature and pressure.

In the modeling work of this paper, efforts were taken to find the dependence of the reversible potential on temperature for low temperature PEM electrolyzers. Experimental *I–V* characteristics obtained from a 6 kW PEM electrolyzer stack were modeled using Mathematica programming software. Nonlinear curve fitting algorithms were utilized to extract the critical parameters such as anode and cathode exchange current densities and membrane conductivity. Temperature dependent equations for the reversible potential along with equations for activation and ohmic losses from the literature were used to model the experimental *I–V* data.

LeRoy and Bowen [7] have described the thermodynamics of water electrolysis assuming hydrogen, oxygen, and water vapor behave as ideal gases. The enthalpy of water dissociation reaction is expressed as follows:

$$\Delta H_{t,p} - \Delta H_{25}^0 = [\Delta H_t^0 - \Delta H_{25}^0] + [\Delta H_{t,p} - \Delta H_t^0] \quad (2)$$

where

$$\Delta H_t^0 - \Delta H_{25}^0 = [\Delta H_t^0 - \Delta H_{25}^0]_{H_2} + 0.5[\Delta H_t^0 - \Delta H_{25}^0]_{O_2} - [\Delta H_t^0 - \Delta H_{25}^0]_{H_2O\ (liq.)} \quad (3)$$

and

$$\Delta H_{t,p} - \Delta H_t^0 = [\Delta H_{t,p} - \Delta H_t^0]_{H_2} + 0.5[\Delta H_{t,p} - \Delta H_t^0]_{O_2} - [\Delta H_{t,p} - \Delta H_t^0]_{H_2O\ (liq.)} \quad (4)$$

In these equations, $t$ is temperature in °C, $p$ is the pressure in atmosphere, and $\Delta H_{25}^0$ is the change in enthalpy at standard temperature and is equal to 285.83 kJ

The value for $\Delta H_t^0 - \Delta H_{25}^0$ in Eq. (3) was calculated for different temperatures using the following equation. [8]

$$\Delta H_t^0 = \langle C_P \rangle_H (T - T_0) \quad (5)$$

where $T$ is temperature in Kelvin and $T_0$ = 298.15 K. $\langle C_P \rangle_H$ is the mean heat capacity and is given by

$$\frac{\langle C_P \rangle_H}{R} = A + \frac{B}{2} T_0(\tau + 1) + \frac{C}{3} T_0^2(\tau^2 + \tau + 1) + \frac{D}{\tau T_0^2} \quad (6)$$

where

$$\tau \equiv \frac{T}{T_0}$$

$R$ is the universal gas constant and the coefficients $A$, $B$, $C$ and $D$ for hydrogen, oxygen and water were obtained from the thermodynamic tables for heat capacities for gases and liquid water [8]. The value for $\Delta H_t^0 - \Delta H_{25}^0$ was calculated using these values at different temperatures. $\Delta H_t^0 - \Delta H_{25}^0$ was found to decrease with temperature and can be modeled as a function of temperature t in °C as

$$\Delta H_t^0 - \Delta H_{25}^0 = 741.07 - 51.364t - 0.0633t^2 \quad (7)$$

The effect of temperature and pressure on the enthalpy of water electrolysis reaction can be seen as an enthalpic voltage and can be expressed as [7]

$$V_t = \frac{\Delta H_t^0}{nF} \quad (8)$$

Substituting for $\Delta H_t^0$ from Eq. (7), $V_t$ can be represented as

$$V_t = 1.4850 - 2.6617 \times 10^{-4} t - 3.2803 \times 10^{-7} t^2 \quad (9)$$

Also, the higher heating value voltage ($V_{HHV}$) is defined as [7]

$$V_{HHV,t} = V_t + (\Delta H_t^0 - \Delta H_{25}^0)_{H_2O\ (liq.)}/nF \quad (10)$$

where $(\Delta H_t^0 - \Delta H_{25}^0)_{H_2O\,(liq.)}$ was evaluated using Eqs. (5) and (6) and can be represented as a function of temperature as

$$(\Delta H_t^0 - \Delta H_{25}^0)_{H_2O\,(liq.)} = -1755.8 + 121.9t + 0.1367t^2 \quad (11)$$

Then, $V_{HHV,t}$ can also be represented as a temperature function by substituting Eq. (11) in Eq. (10) as follows

$$V_{HHV,t} = 1.4759 + 3.6553 \times 10^{-4}t + 3.8037 \times 10^{-7}t^2 \quad (12)$$

Eq. (12) can predict the values of $V_{HHV}$ at respective temperatures to evaluate the $V_{HHV}$ based energy efficiency of electrolyzers.

In addition to temperature, the emf ($E$) of an electrolyzer cell producing wet hydrogen and wet oxygen is also affected by the concentrations of products and reactants. Considering the pressure effects of these gases, the emf of the cell, or the Nernst potential, is given by

$$E_{Nernst} = E_{rev}^0 + \frac{RT}{nF} \ln\left(\frac{P_{H_2}P_{O_2}^{0.5}}{P_{H_2O}}\right) \quad (13)$$

where $E_{rev}^0$ is the reversible potential without the effect of pressures. In terms of electrical energy supplied to the electrolyzer, Eq. (13) can be written as

$$nFE_{Nernst} = nFE_{rev}^0 + RT \ln\left(\frac{P_{H_2}P_{O_2}^{0.5}}{P_{H_2O}}\right) \quad (14)$$

where for a given temperature,

$$nFE_{rev}^0 = [G_{f,H_2}^0 + 0.5G_{f,O_2}^0 - G_{f,H_2O\,(liq.)}^0] = -\Delta G_{f,H_2O\,(liq.)}^0 \quad (15)$$

where $G_f^0$ is the standard Gibbs free energy of formation. The change in standard Gibbs' free energy of formation of liquid water ($\Delta G_{f,H_2O\,(liq.)}^0$) at 25 °C (298.15 K) is −237.129 kJ and so the value of $E_{rev}^0$ at 25 °C results in 1.2291 V.

From thermodynamic principles [7]

$$\frac{\partial(G/T)}{\partial T} = -\left(\frac{H}{T^2}\right) \quad (16)$$

$$\frac{\partial(E_{rev}^0/T)}{\partial T} = -\left(\frac{V_t}{T^2}\right) \quad (17)$$

Substituting the value of $V_t$ from Eq. (9) into Eq. (17) and rearranging,

$$E_{rev}^0 = 1.5241 - 1.2261 \times 10^{-3}T + 1.1858 \times 10^{-5}T\ln(T) + 5.6692 \times 10^{-7}T^2 \quad (18)$$

For this work, the partial pressure of hydrogen was calculated based on the total pressure at the cathode ($1 \times 10^6$ N m$^{-2}$) and the assumption that the partial pressure of liquid water is equal to its saturated vapor pressure at the given temperature. An assumption is also made that only water vapor and hydrogen exist in the gaseous phase at the cathode and only oxygen and water vapor are present in the gaseous phase at the anode. The total pressure at the anode was assumed to be constant at $1 \times 10^5$ N m$^{-2}$. Also, the solubility of hydrogen and oxygen in water are assumed negligible. Ideal behavior of these gases is assumed because of low pressure, hence applying the Dalton's law of partial pressures;

$$P_{O_2} = P_{Anode} - P_{H_2O} \quad (19)$$

$$P_{H_2} = P_{Cathode} - P_{H_2O} \quad (20)$$

The total electrolyzer cell voltage can be represented as

$$E_{Total} = E_{Nernst} + E_{Activation} + E_{Ohmic} \quad (21)$$

where $E_{Nernst}$ is given by Eq. (13) and $E_{Activation}$ is the activation overpotential that electrochemical reaction has to overcome for the conversion of reactants to products. This $E_{Activation}$ is modeled by the Butler–Volmer equation [9]. However, the equation for activation overpotential for this work is not used in its traditional form. The hyperbolic sine approximation to the Butler–Volmer equation used in this work because the hyperbolic form is relatively easy to model using nonlinear curve fitting algorithms [4,6]. If one of the exchange current densities (i.e., anode or cathode) is sufficiently larger than the other, then the corresponding activation loss can be neglected [10]. However, for the purpose of extracting the exchange current densities at the anode and cathode from the experimental data obtained for a 6 kW PEM electrolyzer, activation losses at both the electrodes are considered.

$$E_{Activation} = \frac{RT}{2\alpha_A F}\sinh^{-1}\left(\frac{j}{2j_{A,o}}\right) + \frac{RT}{2\alpha_C F}\sinh^{-1}\left(\frac{j}{2j_{C,o}}\right) \quad (22)$$

where $j$ is the current density, $j_{A,o}$ and $j_{C,o}$ are the exchange current density at the anode and cathode, respectively. $\alpha_A$ and $\alpha_C$ are the charge transfer coefficients (CTC) at the anode and cathode, respectively. The CTC at the cathode is set at 0.5, but the CTC values at the anode have been observed to be a function of temperature and its mean value was used at respective temperatures [11].

The ohmic overpotential, $E_{Ohmic}$, due to the membrane resistance, is given by

$$E_{Ohmic} = \frac{\varphi}{\sigma}j \quad (23)$$

where $\varphi$ is the dry thickness of the electrolyte–membrane (178 μm for Nafion™117), and $\sigma$ is the conductivity of the membrane (S cm$^{-1}$).

Substituting for $E_{Nernst}$, $E_{Activation}$, and $E_{Ohmic}$ in Eq. (21) results in Eq. (24). This semiempirical equation is used to model the experimental $I$–$V$ data at different temperatures.

$$E_{Total} = E_{rev}^0 + \frac{RT}{2F}\ln\left(\frac{P_{H_2}P_{O_2}^{0.5}}{P_{H_2O}}\right) + \frac{RT}{2\alpha_A F}\sinh^{-1}\left(\frac{j}{2j_{A,o}}\right) + \frac{RT}{2\alpha_C F}\sinh^{-1}\left(\frac{j}{2j_{C,o}}\right) + \frac{\varphi}{\sigma}j \quad (24)$$

where $E_{rev}^0$ is given by Eq. (18) as a function of temperature.

Generally, the electrolyzer electrical efficiency ($\eta$) is calculated based on the higher heating value voltage using the following equation:

$$\eta = \frac{V_{HHV,t}}{V_C} \quad (25)$$

Electrical efficiency is more important than the heat-energy efficiency in terms of the cost of hydrogen production, so research should be focused on reducing the reversible voltage to bring it closer to the thermoneutral voltage ($V_{tn}$), enthalpic voltage ($V_t$), or higher heating value voltage ($V_{HHV,t}$) [2]. This can be achieved by reducing the activation losses and ohmic losses.

## 4. Results and discussion

Reversible potential without the effect of pressure ($E_{rev}^0$) from Eq. (18) and the Nernst potential ($E_{Nernst}$) from Eq. (13) are plotted as a function of temperature in Fig. 2. The reversible potential decreases with temperature. The difference between the reversible voltage based on Gibbs' free energy and Nernst potential represents the concentration effects of products and reactants. The difference between these two potentials represents the irreversibilities of the system. Higher temperatures favor the electrolysis reaction, as

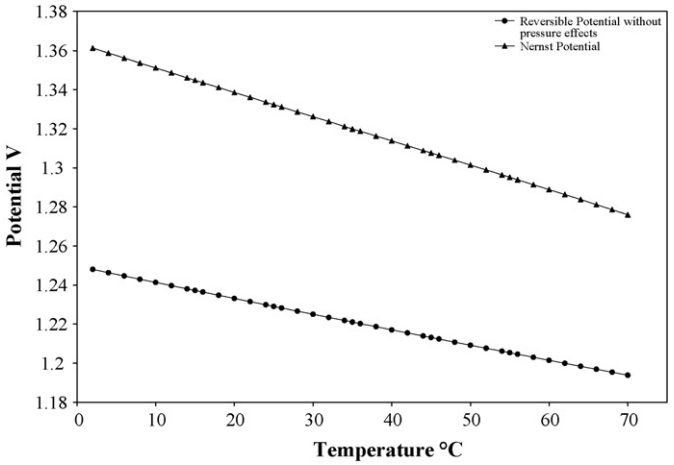


**Fig. 2.** The influence of pressure and temperature on the reversible potential of an electrolysis cell.

shown in Fig. 2, by decreasing the Nernst potential with increasing temperature.

The average cell voltage was calculated from the measured stack voltage using the *I–V* characteristics obtained for various temperatures. As can be seen from Fig. 3, the actual cell voltage is higher than higher heating value voltage at low temperatures, resulting in low electrical energy efficiency. The cell voltage decreases as the temperature increases which brings cell voltage closer to the higher heating value voltage resulting in high electrical energy efficiency. This confirms that electrolyzers perform better at higher temperatures. In the case of PEM electrolyzers, the operating temperature is one of the big constraints because of membrane properties. To improve the efficiency, the cell voltage should be as close as possible to the higher heating value voltage. This can be achieved by reducing the ohmic resistance using a thinner membrane and by reducing activation losses using better manufacturing processes, material development, and catalyst loading. Reducing heat losses is also required to approach the thermoneutral voltage. The efficiency and performance of PEM water electrolysis can be improved by optimizing the electrocatalysis properties such as active surface area, specific gravity, electronic resistance, and particle/layer structure [12].

The efficiencies shown in Fig. 3 were calculated using experimental cell voltages and a constant value of the higher heating

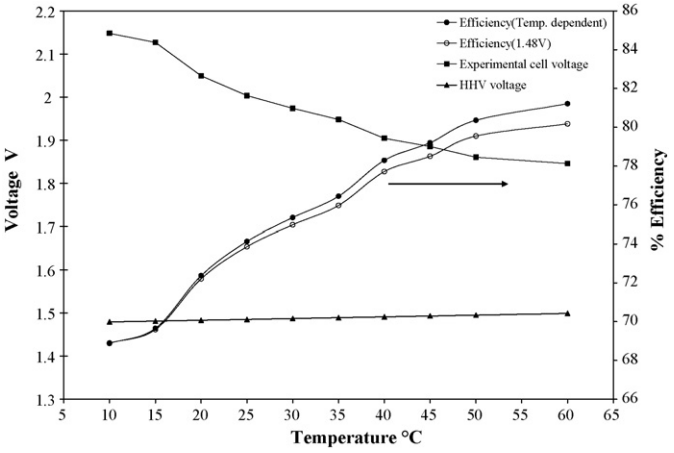


**Fig. 3.** Variation of experimental cell voltage and higher heating value voltage with temperature and electrical energy efficiency at various temperatures at 100 A dc.

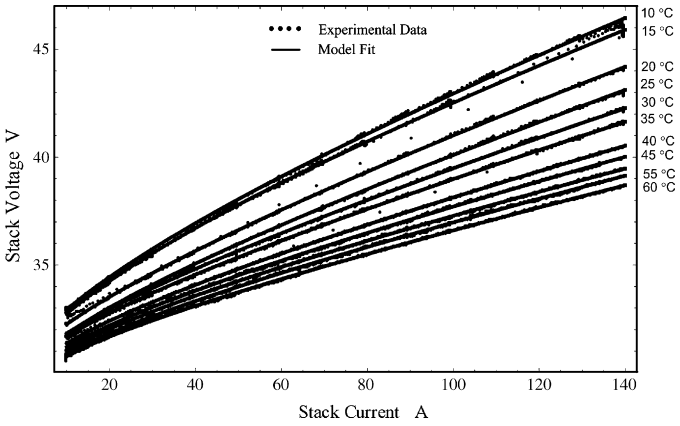


**Fig. 4.** Fitted model with experimental *I–V* data at different temperatures.

value voltage (1.48 V) as well as the $V_{HHV}$ voltage as a function of temperature. A clear difference in efficiencies (Efficiency (1.48 V) and Efficiency (Temp. dependent)) was observed at higher temperatures using different values for $V_{HHV}$. This shows that the use of constant $V_{HHV}$, 1.48 V, may result in a lower efficiency calculation at higher temperatures for PEM electrolyzers.

Nonlinear curve fitting, based on the least square method, was used to fit the experimental *I–V* characteristics to determine the exchange current densities at both electrodes and the membrane conductivity as a function of temperature. The NonLinearRegress function in Mathematica was used to extract the coefficients for the semiempirical Eq. (24) using experimental data. NonLinearRegress uses the Levenberg–Marquardt algorithm [13]. The results were also verified with the FindFit function of Mathematica which also uses a nonlinear curve fitting algorithm. The experimental *I–V* data at different temperatures were modeled using Eq. (24) at respective temperatures. The experimental data for the UND's 6 kW PEM electrolyzer system at different temperatures with the fitted models at respective temperatures is shown in Fig. 4. The temperatures have ±0.2 °C error margin and for simplicity they have been rounded to whole numbers. The CTC value for the cathode is assumed to be equal to 0.5 while fitting the semiempirical equation with the experimental data. As explained earlier, the anode charge transfer coefficient has been found to vary with temperature [11]. The CTC value for the anode had been reported to vary from 0.1 to 0.6 [9,14]. The varying CTC value for the anode was used for this modeling.

Electrolyzer stack parameters such as the anode and cathode exchange current densities were employed as equation coefficients for modeling the experimental *I–V* characteristics. The extracted parameters from the modeling efforts are summarized in Table 1. Both the anode ($j_{A,o}$) and cathode ($j_{C,o}$) exchange current densities showed an upward trend with increasing temperature which agrees

**Table 1**
Extracted parameters from modeling experimental data

| Temperature (°C) | $j_{A,o}$ ($\times 10^{-5}$ A cm$^{-2}$) | $j_{C,o}$ (A cm$^{-2}$) | $\sigma$ (S cm$^{-1}$) |
|---|---|---|---|
| 10 | 0.76 | 0.18 | 0.058 |
| 15 | 1.11 | 0.14 | 0.060 |
| 20 | 1.45 | 0.27 | 0.063 |
| 25 | 2.93 | 0.21 | 0.065 |
| 30 | 2.00 | 0.32 | 0.073 |
| 35 | 2.32 | 0.23 | 0.073 |
| 40 | 3.29 | 0.26 | 0.085 |
| 45 | 3.87 | 0.24 | 0.087 |
| 50 | 4.21 | 0.24 | 0.092 |
| 55 | 4.80 | 0.32 | 0.093 |
| 60 | 4.93 | 0.39 | 0.096 |

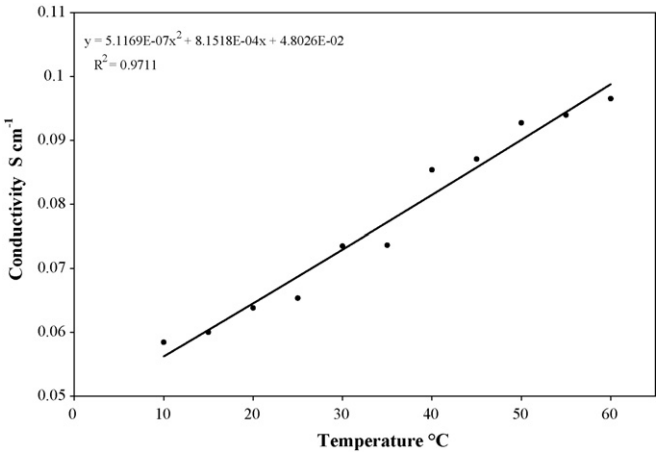


**Fig. 5.** Variation of membrane conductivity with temperature.

with the literature[15]. For platinum based electrodes, the exchange current density at the oxygen electrode is $10^{-9}$ to $10^{-12}$ A cm$^{-2}$ and that of the hydrogen electrode is $1 \times 10^{-3}$ A cm$^{-2}$ [10]. The exchange current density depends on the electrochemically active surface area and the temperature at the electrode surface. The values in Table 1 for the exchange current densities at the hydrogen (cathode) and oxygen (anode) electrodes showed close agreement with the literature values [6,9,10].

The membrane conductivity, $\sigma$, was found to increase with temperature as mentioned in the literature [16]. Fig. 5 shows a linear increase in conductivity with temperature. This rise in conductivity was modeled as a function of temperature in °C and can be represented by

$$\sigma = 0.0480257 + 8.15178 \times 10^{-4}t + 5.11692 \times 10^{-7}t^2 \quad (26)$$

The nonlinear curve fitting algorithm method with the semiempirical Eq. (24) developed in this work allows the proprietary values of membrane thickness, conductivity, and the anode and cathode exchange current densities to be determined from experimental *I–V* characteristics. The use of temperature and pressure dependent Nernst potential in the semiempirical equation helps in obtaining more accurate determination of the electrolyzer cell and stack parameters. The higher heating value voltage, reversible voltage, and Nernst voltage when represented as a function of temperature, can help in future simulations to obtain physically more significant *I–V* characteristics at different operating conditions.

## Acknowledgements

This work is sponsored by the US Department of Energy and the North Dakota Experimental Program to Stimulate Competitive Research (NDEPSCoR) under Grant No. DE-FG 02-04-ER46115 and the National Science Foundation Research Infrastructure Improvement under Grant No. ESP-0447679.

## References

[1] J. Ivy, NREL/MP-560-36734 (2004) (Website: http://www.nrel.gov/docs/fy04osti/36734.pdf), Website last accessed on April 21, 2008.
[2] A. Roy, S. Watson, D. Infield, Int. J. Hydrogen Energy 31 (2006) 1964–1979.
[3] K. Onda, T. Murakami, T. Hikosaka, M. Kobayashi, R. Notu, K. Ito, J. Electrochem. Soc. 149 (2002) A1069–A1078.
[4] P. Choi, D.G. Bessarabov, R. Datta, Solid State Ionics 175 (2004) 535–539.
[5] http://www.distributed-energy.com.
[6] K.W. Harrison, E. Hernandez-Pacheco, M. Mann, H. Salehfar, J. Fuel Cell Sci. Technol. 3 (2006) 220–223.
[7] R.L. LeRoy, C.T. Bowen, J. Electrochem. Soc. 127 (1980) 1954–1962.
[8] J.M. Smith, H.C. Van Ness, M.M. Abbott, Introduction to Chemical Engineering Thermodynamics, McGraw-Hill Publ., 2003.
[9] J. Larminie, A. Dicks, Fuel Cell Systems Explained, 2nd ed., John Wiley & Sons Ltd., England, 2003.
[10] D.A. Noren, M.A. Hoffman, J. Power Sources 152 (2005) 175–181.
[11] C.Y. Biaku, N.V. Dale, M.D. Mann, H. Salehfar, T. Han, Int. J. Hydrogen Energy 33 (2008) 4247–4254.
[12] A. Marshall, B. Borresen, G. Hagen, M. Tsypkin, R. Tunold, Energy 32 (2007) 431–436.
[13] H. Ruskeepaa, Mathematica Navigator, 2nd ed., Elsevier Academic Press, 2003.
[14] A. Parthasarathy, S. Srinivasan, A.J. Appleby, J. Electrochem. Soc. 139 (1992) 2530–2537.
[15] K. Harrison, Design, Integration and Control of Proton Exchange Membrane Electrolyzer for Wind Based Renewable Energy Application, Dissertation, University of North Dakota, August 2006.
[16] T. Springer, T. Zawodzinki, S. Gottesfeld, J. Electrochem. Soc. 138 (1991) 2334–2342.